OPEN

Nanoliter-Scale Protein Crystallization and Screening with a Microfluidic Droplet Robot

Ying Zhu[1], Li-Na Zhu[1], Rui Guo[2], Heng-Jun Cui[2], Sheng Ye[2] & Qun Fang[1]

[1]Institute of Microanalytical Systems, Department of Chemistry, Zhejiang University, Hangzhou, 310058, China, [2]Life Sciences Institute, Zhejiang University, Hangzhou, 310058, China.

Large-scale screening of hundreds or even thousands of crystallization conditions while with low sample consumption is in urgent need, in current structural biology research. Here we describe a fully-automated droplet robot for nanoliter-scale crystallization screening that combines the advantages of both automated robotics technique for protein crystallization screening and the droplet-based microfluidic technique. A semi-contact dispensing method was developed to achieve flexible, programmable and reliable liquid-handling operations for nanoliter-scale protein crystallization experiments. We applied the droplet robot in large-scale screening of crystallization conditions of five soluble proteins and one membrane protein with 35–96 different crystallization conditions, study of volume effects on protein crystallization, and determination of phase diagrams of two proteins. The volume for each droplet reactor is only *ca.* 4–8 nL. The protein consumption significantly reduces 50–500 fold compared with current crystallization stations.

X-ray crystallography has revolutionized our knowledge on macromolecular behaviors and functions[1–3], and plays an important role in the study of protein–ligand interactions[4], the rational design of novel drug candidates[3,5], and the in-depth understanding of human diseases[6]. With the successful structural determination of many proteins, current efforts mainly focus on membrane proteins and protein complexes. However, working on these biologically-important macromolecules is challenging, as they are difficult to be overexpressed and purified, and are usually available only in sub-milligram quantities[7,8]. The situation becomes more severe for those that cannot be overexpressed in model organisms and must be purified from nature. Despite the tremendous advances in X-ray radiation sources, data processing strategies and relative technologies, obtaining high-quality crystals suitable for X-ray diffraction remains the main rate-limiting step in structure determination process[9]. Each protein crystallizes at a specific and narrow chemical condition where nucleation and crystal growth occur. Unfortunately, no theoretical approaches are available to predict such condition for unknown proteins at the present time. Large-scale screening by searching hundreds, or even thousands of chemical conditions involving various salts, buffers, and precipitating agents remains the main approach[10,11], which requires a large amount of sample at milligram level, and thus is unrealistic for many scarce protein targets. In recent years, there has been a growing interest to minimize crystallization trials in nanoliter-scale volumes with the state-of-art liquid handling tools, since nanoliter-scale trial allows for more comprehensive screening of chemical conditions with sub-milligram amount of protein samples, and thus significantly reduces the cost and time of crystallization screening[12–15].

Current minimization technologies for protein crystallization have been focused on two independent strategies: automated robotics integrated with micro-dispensing heads[14,15], or microfluidic chips with parallel valves or water-in-oil droplets[12,13]. The automated robots, such as Phoenix (Art Robbins Instruments, Inc.), Mosquito (TTP Labtech, Ltd.), and OryxNano (Douglas Instruments, Ltd.) are capable of dispensing and mixing protein and crystallization solutions to the smallest volumes of 25–100 nL. With the advantages of low sample consumption, high reliability, high throughput, and complete automation, these robots are extensively advocated in structural biology laboratories. Other types of robotics[16], such as pin tool[17] and acoustic dispensing[18], with the ability of processing nanoliter- or even picoliter-scale liquid, although widely applied in DNA or protein micro-array chip preparations, lack application in protein crystallization experiments, mainly because such liquid handling methods are highly sensitive to the liquid properties such as surface tension and viscosity[16], and the situation becomes more severe when the liquid volume is in sub-nanoliter scale. Thus, automated robotics capable

of reliably performing protein crystallization trials with volumes of sub-nanoliter to several nanoliters is not available at the present time.

Microfluidic techniques have been applied to protein crystallization in both screening and optimization stages[12,13]. With specially-designed microchannels, valves, and chambers, microfluidic devices have intrinsic abilities to generate and manipulate small volumes of liquids, enabling various types of crystallization trials within these devices. One example was reported by Hansen et. al.[8], where nanoliter-scale protein and crystallization solutions were metered and filled into volume-defined microchambers, and were then allowed to diffusively mix with each other using an array of pneumatic valves. By integrating multiple groups of microvalves on a chip, the same group developed a formulation chip for rapidly generating and actively mixing complex mixtures of protein and crystallization solution, and used it to study protein phase behavior[19,20]. Another simple but efficient example was described by Zheng et.al.[21], where a T junction channel was used to generate nanoliter-scale water-in-oil droplets containing mixtures of protein and crystallization solutions, and the mixing ratios were adjusted by changing the corresponding flow rates. Such a method can be regarded as a miniaturized micro-batch, but the droplet volumes are smaller than traditional ones. For sparse matrix screening, an array of droplets containing different crystallization solutions was loaded into a capillary and then merged with a protein solution in a T junction channel[22]. A recent example termed as SlipChip was developed by Du et. al.[23,24], where different crystallization solutions were loaded in the wells of the bottom plate and a protein sample was loaded in the channels of the top plate. The top plate was then slipped to mix protein solution with crystallization solutions to form crystallization trials. Another noteworthy microfluidic technique is PhaseChip[25,26], where hundreds of nanoliter-scale droplets can be spontaneously trapped and stored in microwells using surface tension force. The PhaseChip is suitable for mapping the phase diagrams of protein crystallization[25] and precisely controlling the nucleation and crystal growth process[26]. However, despite the transformative potentials of microfluidic techniques for protein crystallization, broad adoption and use of these techniques for real samples have been lagged, mainly due to two reasons. One reason may be that the design, fabrication, and operation of microfluidic devices require specific equipment and technical training[27], which are not available in most of the structural biology laboratories. In addition, compared with conventional crystallization robots, microfluidic systems still require many manual operations, such as pipetting solutions from sample reservoirs to microchips.

Here, we describe a fully automated droplet robot for nanoliter-scale protein crystallization screening that combines the automated robotics technique for protein crystallization screening with the droplet-based microfluidic technique. It can achieve flexible and programmable liquid handling operations for various protein crystallization experiments in the scale ranging from several nanoliters to sub-nanoliters, including large-scale protein crystallization screening, study of protein crystallization behaviors, and determination of the phase diagrams for proteins. The droplet robot was built using commercially available modules and microdevices, and can be produced by simple microfabrication techniques and equipment, on the basis of the design strategy of sequential operation droplet array (SODA)[28]. A tapered capillary (20–30 μm tip size) connected to a commercial syringe pump with picoliter-scale precision was used for nanoliter-scale liquid metering, aspirating and dispensing[28–30]. A nanowell array chip (Figure 1a1) fabricated using standard photolithography and wet chemical etching techniques and covered with a layer of oil to reduce droplet evaporation, serves as containers of protein crystallization droplet reactors with a high density of 676 droplets/cm² (Figure 1a2). The microchip and a commercial 384-well plate containing proteins and crystallization solutions are fixed on an x-y-z translational stage with micrometer-scale precision. Various liquid handling operations are performed by using the synchronous control of the syringe pump and the x-y-z stage according to computer programs. We have investigated the liquid-handling methodology suitable for nanoliter-scale protein crystallization screening with a variety of liquid types and large variations in liquid viscosity and surface tension, and developed a novel semi-contact dispensing method to achieve reliable and continuous droplet generation and sample/reagent addition. In this work, we applied the droplet robot in large-scale crystallization screenings of five soluble proteins and one membrane protein with 35–96 different crystallization conditions, study of volume effects on protein crystallization, and determination of the phase diagrams of two proteins, with ca. 4–8 nL volume for each droplet reactor.

The liquid-handling operation of the droplet robot is schematically shown in Figure 1. For screening of multiple crystallization conditions, a precipitant droplet array containing all kinds of tested precipitants is first generated (Figure 1b1). The precipitant droplet is formed by moving the x-y-z stage to allow the capillary tip to aspirate definite volume (2–4 nL) of a crystallization solution into the capillary using the syringe pump. The x-y-z stage is then moved to align the capillary tip on the top and center of a nanowell of the microchip, allowing the syringe pump to push the precipitant solution out from the capillary tip and deposit it in the nanowell. The droplet array for crystallization trials is generated by sequentially adding a definite volume (2–4 nL) of the target protein solution into each preformed precipitant droplet and mixed with the precipitant, respectively (Figure 1b2). For the study of protein solubility behaviors for definite precipitants (Figure 1c), three continuously volume-tunable dispensing operations for precipitant, buffer, and protein solutions are required to produce a two-dimensional (2D) phase diagram. In each operation, the liquid dispensing volume is varied according to a program, ensuring the precise control of in-droplet protein and precipitant concentrations in the 2D droplet array. After the droplet array for screening or study is formed, the whole microchip is further sealed with a glass slide to avoid droplet dehydration during long-term crystallization incubation period.

Results

Liquid handling in nanoliter-scale for protein crystallization experiments. In the present droplet robot, the droplet array chip was covered with a layer of oil to reduce the evaporation of nanoliter-scale droplets. In a preliminary study, we observed that conventional micro-scale liquid handling techniques, including contact dispensing and contactless dispensing, are not suitable for handling nanoliter-scale liquids under oil. The contact dispensing technique with the capillary tip end directly contacting the chip surface could lead to the uncontrollable generation of a large number of small droplets, as well as the risk of breaking the capillary tip. The contactless dispensing technique has difficulty in releasing droplets from the capillary tip to the chip wells due to the adhering of the droplets on the capillary tip, which is caused by the weak gravity effect and significant surface effect in a microsystem (Figure 1d2). Thus, we developed the semi-contact dispensing method to achieve reliable and continuous nanoliter-scale droplet generation and sample/reagent addition under oil phase. With the semi-contact dispensing method, the distances between the capillary tip end and the bottom of the chip nanowell (d_1 and d_2 in Figure 1d1 and 1d5) are precisely adjusted according to the size range of dispensed droplets. In droplet generation, such a design allows the dispensed droplet to contact the surface of the nanowell bottom and then to be released from the capillary tip (Figure 1d1–4). For continuous sample/reagent addition into preformed droplet, the distance (d_2) is adjusted to allow the dispensed droplet to contact with the preformed droplet (Figure 1d5,6). Unlike other in-channel droplet-based microfluidic systems, where surfactants are usually added in oil phase to stabilize droplets from being fused[31], no surfactant is used in the present nanowell array droplet system,
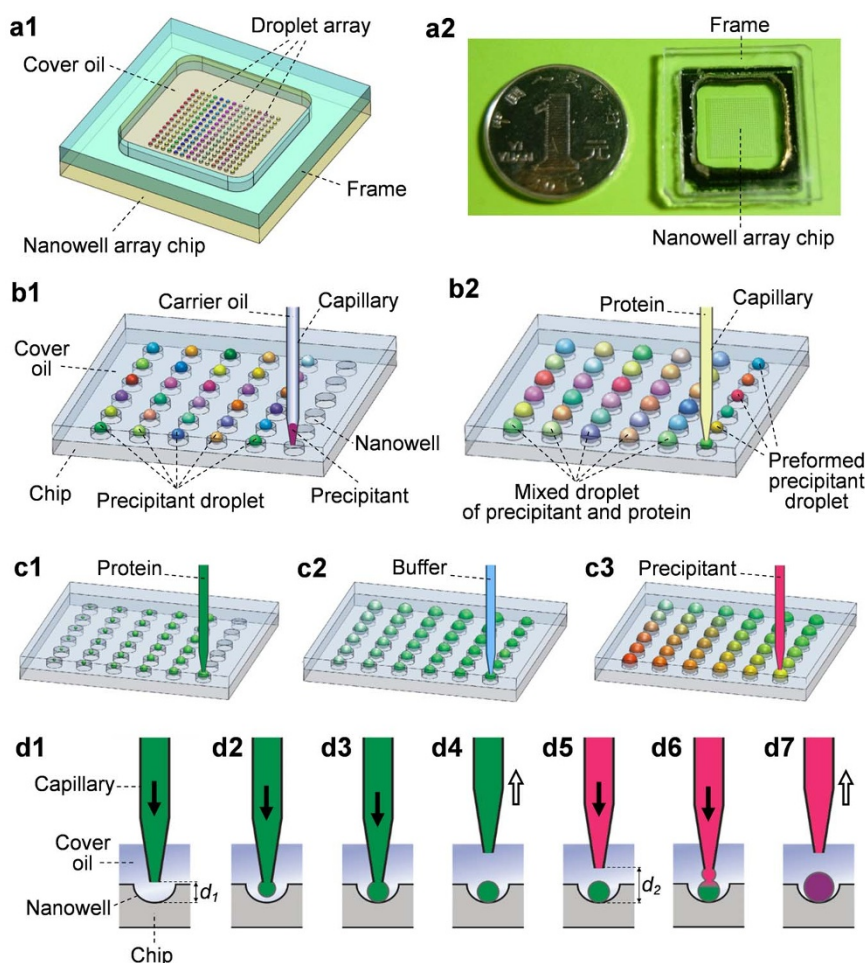
Figure 1 | (a1) Schematic configuration of a nanowell array chip with droplet array. (a2) Image of a prototype microchip with 784 wells. (b) Schematic procedures of generation of precipitant droplets on a nanowell array chip (b1) and addition of protein solution into each precipitant droplet (b2). (c) Schematic procedure for generating a 2D droplet array for determination of protein phase diagram with a given precipitant. (c1) Precipitant is first dispensed on nanowells to form droplets with different volumes. (c2) Buffer solution is sequentially added into the droplets with programmable volumes. (c3) Protein solution is sequentially added into the droplets with programmable volumes. (d) Schematic diagram showing the principle of semi-contact droplet dispensing technique for continuous droplet generation and sample/reagent addition.

and thus the dispensed droplet can be easily merged with the preformed droplet once contacting each other (Figure 1d6). In a more reliable design, the capillary probe tip can be inserted into the preformed droplet to inject definite volume of protein solution with a shorter distance d_2. The nanowell can efficiently maintain the position of droplets during the sample/reagent addition process.

The crystallization reagents have large variations in liquid properties, such as viscosity and surface tension. This is challenging for precise liquid handling, especially on the nanoliter scale. Thus, we first evaluated the performance of the droplet robot in processing nanoliter-scale viscous liquids. An array of 1.98-nL aqueous droplets containing 0%, 10%, 20%, and 30% PEG 6000 (w/v), with a wide range of viscosities as 1.01, 3.40, 5.82, and 10.42 mPa·s, respectively, was generated by the droplet robot (Figure 2a). The corresponding relative standard deviations (RSDs) of droplet diameters were measured as 0.72%, 0.68%, 0.59%, and 0.55% (n = 20) respectively, demonstrating a high precision of the robot in handling nanoliter-volume viscous liquids. The slight increase of droplet diameter proportional to the PEG concentration may be attributed to the decrease of the contact angle of droplets on the microchip surface with the PEG concentration. To test the smallest volume of viscous liquid that the robot can stably and reproducibly handle, we produced an array of droplets containing 30% PEG 6000 (w/v) with gradually decreasing volumes of 1.98 nL, 0.99 nL, 0.48 nL, and 0.12 nL (Figure 2b).

The corresponding RSDs of droplet diameters were 0.71%, 0.74%, 1.96%, and 7.71%, respectively (n = 20). Further generating smaller droplets is unstable and irreproducible with the present system. Two relatively large-scale arrays of 100, 1.98-nL droplets containing 5 mM sodium fluorescein and five different food dyes with diameter RSDs from 0.58% to 1.79% were also produced to demonstrate the ability of the droplet robot to reliably generate a large number of droplets suitable for screening (Figure S1).

In both experiments for crystallization screening and solubility behavior study, two or more reagents need to be sequentially added into and mixed with preformed droplets. The performance of the robot was evaluated in conducting definite-volume liquid addition to preformed droplets. In the first evaluation, an array of 50, 1.98 nL droplets (5 mM sodium fluorescein in 50 mM borate buffer) was formed on the microchip, and a blank buffer solution (50 mM borate) was sequentially added into each droplet with an equal volume of 1.98 nL to dilute the droplets (Figure 2c). The RSDs of the 50 droplets before and after the buffer addition were 1.11% and 1.00%, respectively, showing the high precision in nanoliter-scale reagent addition. In the second evaluation, an array of droplets containing sodium fluorescein with increased concentrations from 1 μM to 9 μM was prepared by changing the mixing ratios of a concentrated sample solution (10 μM sodium fluorescein) and a buffer solution (50 mM borate). A series of droplets with increased
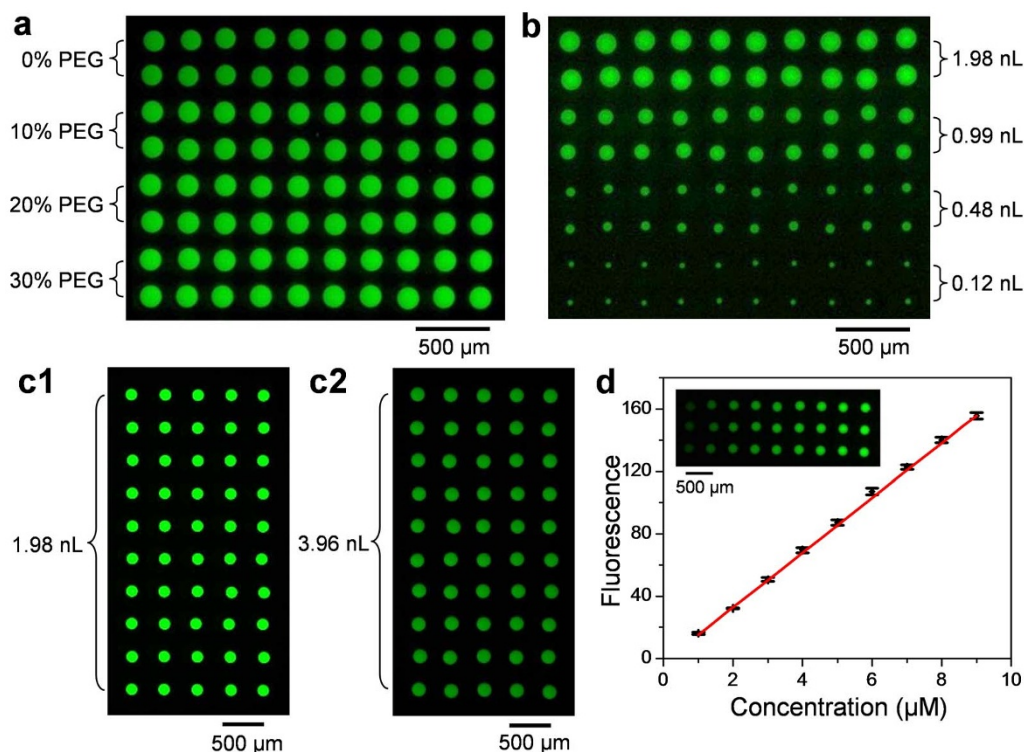
Figure 2 | Performance of the droplet robot in handling nanoliter-volume liquid. (a) Image of an array of aqueous droplets containing 0%, 10%, 20%, and 30% PEG 6000 to show the precision in handling viscous liquids. (b) Image of an array of droplets containing 30% PEG 6000 with volumes of 1.98 nL, 0.99 nL, 0.48 nL, and 0.12 nL. (c) Precision testing of multi-step continuous reagent addition into preformed droplets. An array of 1.98 nL droplets containing 5 mM sodium fluorescein and 30% PEG 6000 is formed (c1), and a buffer solution is dispensed into each droplet with a volume of 1.98 nL to dilute the preformed droplets (c2). (d) Precision testing of continuously volume-tunable dispensing and reagent addition technique. An array of droplets containing sodium fluorescein with concentrations from 1 μM to 9 μM is formed by programmably mixing 10 μM sodium fluorescein solution with a buffer solution (50 mM borate).

volumes from 0.42 to 3.78 nL with an increment of 0.42 nL were first generated by continuously dispensing the sample solution, and then the buffer solution was injected into the corresponding droplets with decreased volumes from 3.78 to 0.42 nL with a decrement of 0.42 nL. The final volume for each droplet was 4.20 nL (Figure 2d). The measured fluorescence intensities show excellent linear relationship with target concentrations over the full range ($R^2 = 0.999$). A relatively large-scale droplet array with 2D concentration gradients of two dyes can be found in Figure S2.

We next tested the cross-contamination of the droplet robot, since a single sampling probe was used to process different samples and reagents. To evaluate the cross contamination between sequentially generated droplets, a series of 1.98-nL droplets containing 10 mM sodium fluorescein and 1.98-nL blank buffer (50 mM borate) droplets were alternately formed, and the fluorescence intensities of the blank droplets were measured. After calibration with standard curves, the average concentration of sodium fluorescein in the contaminated blank droplets was calculated as 1.48 ± 0.15 μM (n = 5), indicating the cross contamination is *ca.* 0.02%. The carryover during continuous reagent addition operations was also tested by first using the capillary tip to inject 1.98-nL buffer into a sample droplet (1.98 nL, 10 mM sodium fluorescein) and then inject the same volume buffer into a blank droplet. The average concentration in blank droplets was measured as 3.14 ± 0.62 μM (n = 5), showing the carryover is *ca.* 0.03%. These ultra-low cross-contaminations can be attributed to the protection effect of oil phase, which effectively isolates sample solutions from the hydrophobic wall surfaces of the capillary tip, and also washed the residues away from the inner and outer walls of the capillary. Based on these results, no capillary washing step was adopted in the following protein crystallization experiments.

Sparse matrix screening of protein crystallization. The droplet robot was used to implement nanoliter-scale sparse matrix screening of protein crystallization conditions for two model proteins, lysozyme and xylanase. A crystal screen kit containing 96 different conditions was selected, and each condition was tested 3 times. In total, 288 crystallization trials were performed for each protein. For each trial, 2.01 nL protein was mixed with 2.01 nL crystallization solution in a droplet. Thus, only a volume of 578.9 nL protein solution was consumed for each screening, which is *ca.* 2 orders of magnitude lower than those of current standard crystallization robots. For lysozyme, we identified five conditions (D3, H3, B10, G10, and G12) that can produce crystals (Figure 3a). To confirm these results, we performed the crystallization experiments for the identified conditions using conventional microbatch technique with a total reactor volume of 2 μL. Although the crystallization volume was scaled up for 500 times, protein crystals still can be formed with conditions same as those of nanoliter droplets (Figure S3). For xylanase, three conditions (E1, E6, and D12) were identified (Figure 3b) and the results were also confirmed with scaling-up experiments (Figure S4). Besides lysozyme and xylanase, crystals of three other soluble proteins, thaumatin, trypsin, and glucose isomerase, were obtained using known crystallization conditions[8], as shown in Figure 4. An additional favorable feature of using nanoliter-scale droplet array for protein crystallization screening is that the crystals can be easily and rapidly identified using a microscope without frequent refocusing, since the optical paths of droplets are much shorter (Figure 3 and Figure 4). Large number of droplet reactors can be visualized in a single microscopic field.

In addition to soluble proteins, we preliminarily validated the feasibility of the droplet robot for crystallization of membrane pro-
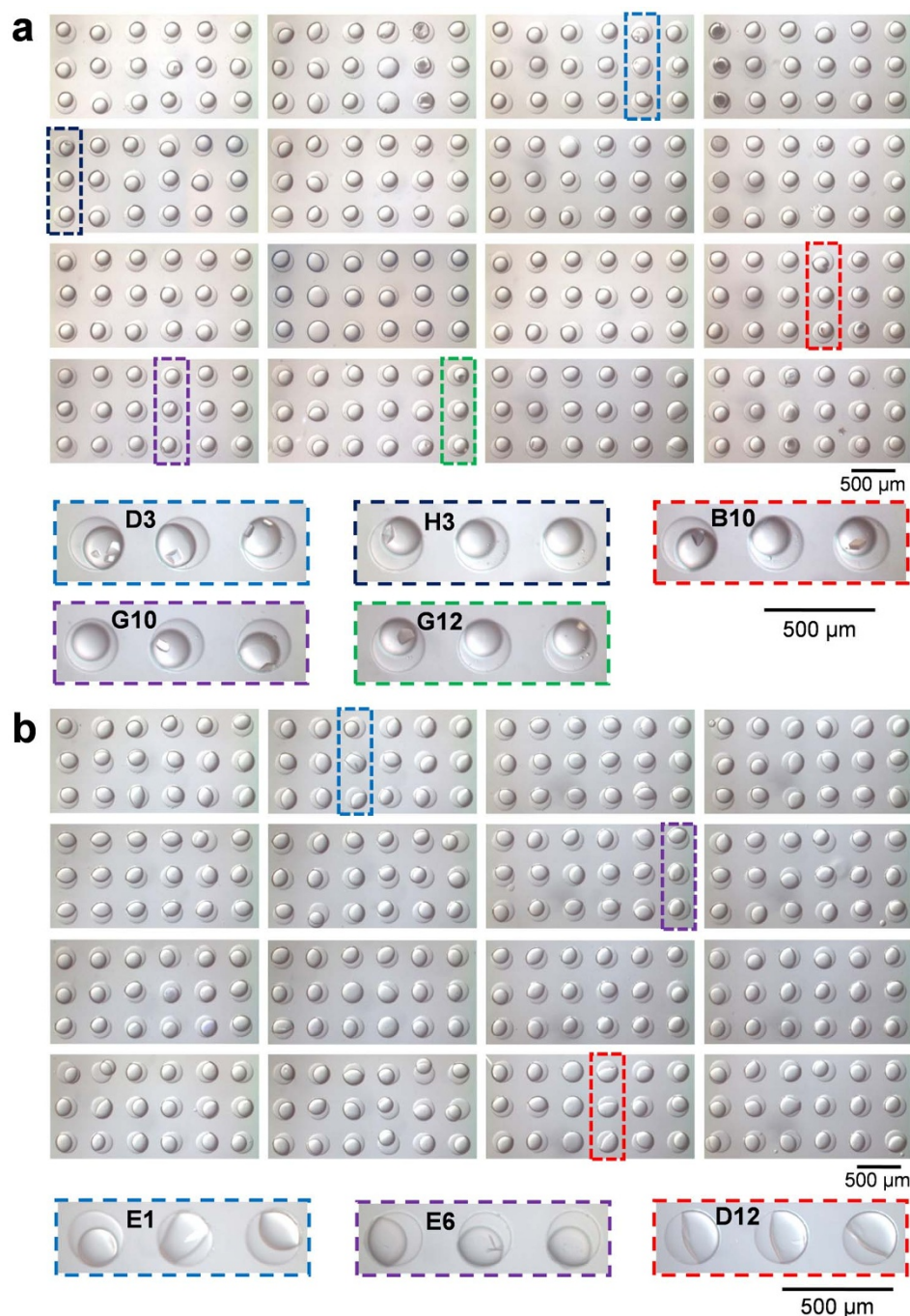
Figure 3 | Large-scale screening of protein crystallization condition in nanoliter-scale droplet array. (a) Combined microscopic image shows the screening result of lysozyme with 96 crystallization conditions (Index HT™ from Hampton). Protein concentration: 50 mg/mL in 0.1 M NaAc buffer (pH 4.6). (b) Combined microscopic image shows the screening result of xylanase with 96 crystallization conditions. Protein concentration: 36 mg/mL in 0.18 M sodium/potassium phosphate buffer (pH 7) containing 43% glycerol (w/v). Each droplet contains 2.01 nL protein and 2.01 nL crystallization solutions, and each condition was repeated three times.

tein. In purifying and solubilizing of membrane proteins, various detergents are necessary to be used, making crystallization solutions have low surface tensions. We first tested the capability of the robot in dealing with low surface tension liquids using a series of aqueous solutions containing different detergents (n-decyl-β-D-maltopyranoside (DM), n-octyl-β-D-glucopyranoside (β-OG), Dimethyl-L-dodecanamine-N-oxide (LDAO), and n-dodecyl-β-D-maltopyranoside (DDM)) with concentrations from 1 mM to 40 mM. For all these solutions, droplets can be reliably generated on chip without observable performance degradation. Then, we chose a model membrane

protein, mechanosensitive channel of large conductance (MscL), to perform crystallization screening experiments. Total 35 crystallization conditions were tested in droplets containing 4.02 nL protein and 4.02 nL crystallization solutions, and after an incubation time of one month, two conditions were identified to be capable of generating needle-like crystals. For the first condition (Figure 4d1), where the protein was solubilized at 20 mg/mL in an aqueous solution with 2 mM LDAO and 3 mM DDM, and the crystallization solution contained 2 M Li_2SO_4, 0.05 M MES (pH5.6), and 0.01 M $MgCl_2$, we also observed similar needle-like crystals in a scaling-up experiment
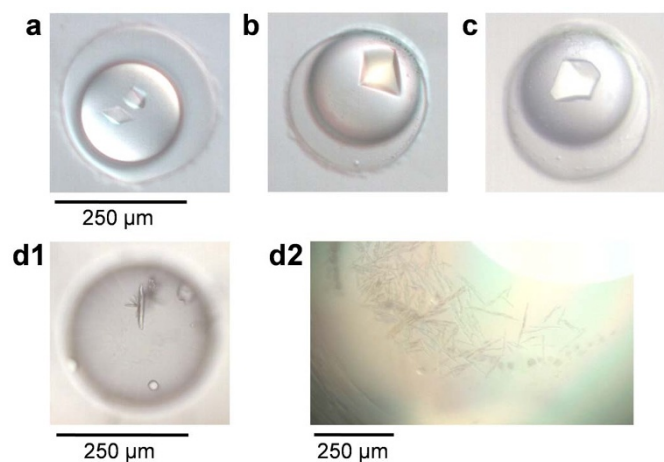
Figure 4 | Microscopic images of droplets with protein crystals of thaumatin (a), trypsin (b), glucose isomerase (c), and MscL (d1). Crystallization conditions: (a) thaumatin: 30 mg/mL in 0.1 M ADA buffer (pH 6.5); Mixing ratio of 1 : 1 with 2 M sodium potassium tartrate in 0.1 M HEPES (pH 7.5). (b) Trypsin: 60 mg/mL in 20 mM HEPES buffer (pH 7.0) containing 10 mM calcium chloride and 10 mg/ml benzamidine hydrochloride; Mixing ratio of 1 : 1 with 0.1 M sodium cacodylate trihydrate buffer (pH 6.5) containing 0.2 M ammonium sulfate and 30% PEG 8,000 (w/v). (c) Glucose isomerase: 19.2 mg/mL in 10 mM HEPES buffer (pH 7.0) containing 1 mM magnesium chloride hexahydrate; Mixing ratio of 1 : 1 with 0.1 M HEPES buffer (pH 7.5) containing 0.2 M calcium chloride dehydrate and 28% PEG 400 (v/v). (d1) MscL: 20 mg/mL in 0.1 M Tris-HCl buffer (pH 7.5) containing 150 mM NaCl, 2 mM LDAO and 3 mM DDM; Mixing ratio of 1 : 1 with 50 mM MES (pH 5.6) containing 2 M Li_2SO_4 and 10 mM $MgCl_2$. (d2) Scale-up crystallization result of MscL using condition as in d1. The crystallization volume is 400 nL containing 200 nL protein and 200 nL precipitant.

(Figure 4d2). For the second condition, where the protein was solubilized at 10 mg/mL in an aqueous solution with 1 mM DDM, and the precipitant solution contained 0.2 M $(NH_4)_2SO_4$ and 40% MPD, no crystal was observed in a scaling-up experiment.

In the present screening experiments, each crystallization condition was tested for 3 times. It is worth noting that the protein crystal nucleation is a stochastic process. The situation is more severe when protein crystallization is performed in nanoliter-scale volumes, where the probability of crystal nucleation is significantly reduced due to reduced interface (see the section of *Volume effect of protein crystallization*). Thus, during real applications, five to ten-fold repetitions for each experimental setting should be used to help to identify more crystallization conditions.

Volume effect of protein crystallization. With the ability in flexibly generating droplets in the picoliter to nanoliter range of the present system, we comprehensively studied the effect of droplet volumes on the behavior of protein crystallization. Crystallization trials for two model proteins (lysozyme and thaumatin) with known crystallization conditions were performed in a series of volumes in the range from 840 pL to 40.08 nL, as well as the volume of 4 μL as in traditional protein crystallization systems. As shown in Figure 5 and Figure S5, proteins crystallize in all these droplets, demonstrating that protein crystallization conditions are similar among the macroscopic and microscopic volumes. On the basis of these results, it is possible to perform screening experiments in picoliter-scale volumes to further reduce the sample consumption in the screening procedure. Differing from large volume droplets, fewer crystals formed in small volume droplets. For both lysozyme and thaumatin, only one crystal was observed in the droplets of 840 pL and 2.04 nL, and more crystals appeared with the increase of the

droplet volume. For thaumatin, protein precipitation (Figure S5b) that occurred in 4-μL droplet was not observed in nanoliter-scale droplets. We also observed three empty droplets in five 840 pL thaumatin droplets. Such phenomena could be explained by that the probability of nucleation events decreases with the reduction of droplet volumes[32]. Indeed, we observed that the chance of crystal formation became lower in smaller droplets from an experiment of a long-term monitoring for lysozyme (Figure S6). For droplets larger than 20 nL, crystals appeared within short incubation time of 30 min. While for droplets smaller than 11 nL, no crystals could be observed within an incubation time of 9.5 h, and crystals appeared in these droplets after a long period of 30 h. These results suggest that varying the nanoliter-scale droplet volume can provide an efficient way to control the nucleation of protein crystallization.

Investigation of protein phase behavior. The protein crystallization process can be illustrated with a 2D phase diagram, which shows different protein phase behaviors (undersaturation, metastable, nucleation, and precipitation) under given chemical parameters including the concentrations of protein and precipitant. Well-order crystals could be formed in a lower supersaturation region, where only limited nucleations take place and the crystals are allowed to grow steadily[9]. Thus, understanding protein phase behavior is essential to design and implement crystallization optimization experiments. However, the current knowledge on protein phase behaviors is limited to some well-known model proteins, which could be attributed to the large amounts of protein sample required by conventional techniques for investigation of protein phase behavior. To address this challenge, several microfluidic approaches have been developed to obtain protein phase diagrams using minimal protein samples. One of these approaches is based on programmable control of multiple microvalves and micropumps on PDMS chips to achieve combinatorial mixing of protein, buffer, and precipitant[19,20]. The other one is based on the controllable generation of composite droplets using external electromagnetic valves[33].

Herein, the droplet robot was used to produce a droplet array with linearly increased protein and precipitant concentrations in two dimensions under the continuous volume-tunable dispensing mode. A 9 × 9 droplet array with a volume of 8.4 nL for each droplet and 2D stepwise-increased concentration gradients with 1–5 fold variation can be generated within 9 min. The total consumption of protein solution was significantly reduced to *ca.* 205 nL. After incubation for two days, different protein phase behaviors were clearly observed in the droplet array including undersaturation, nucleation and crystal growth, and precipitation (Figure 6a1 and 6b1). Considering the stochastic nucleation behaviors, we generated each phase diagram from at least two parallel crystallization experiments. As shown in Figure 6a2 and b2, the two proteins show different patterns. The nucleation zone is broader for lysozyme, while it is narrower for thaumatin. Lysozyme crystallizes in the regions where both protein concentration and precipitant concentration are high, while thaumatin crystallizes in the region where protein concentration is low and precipitant concentration is high. In most regions of the phase diagram, thaumatin crystals appear accompanied with precipitation in droplets. Such a result indicates that controlling the mixing of thaumatin with its precipitant is crucial to avoid precipitation and thus to produce large-size crystals.

Discussion

Here we demonstrated that the droplet robot serves as a versatile and fully-automated platform for nanoliter-scale protein crystallization and screening. Compared with current crystallization stations, it significantly reduces the protein consumption by 50–500 fold[8,11], which is highly valuable for the crystallization of protein targets with
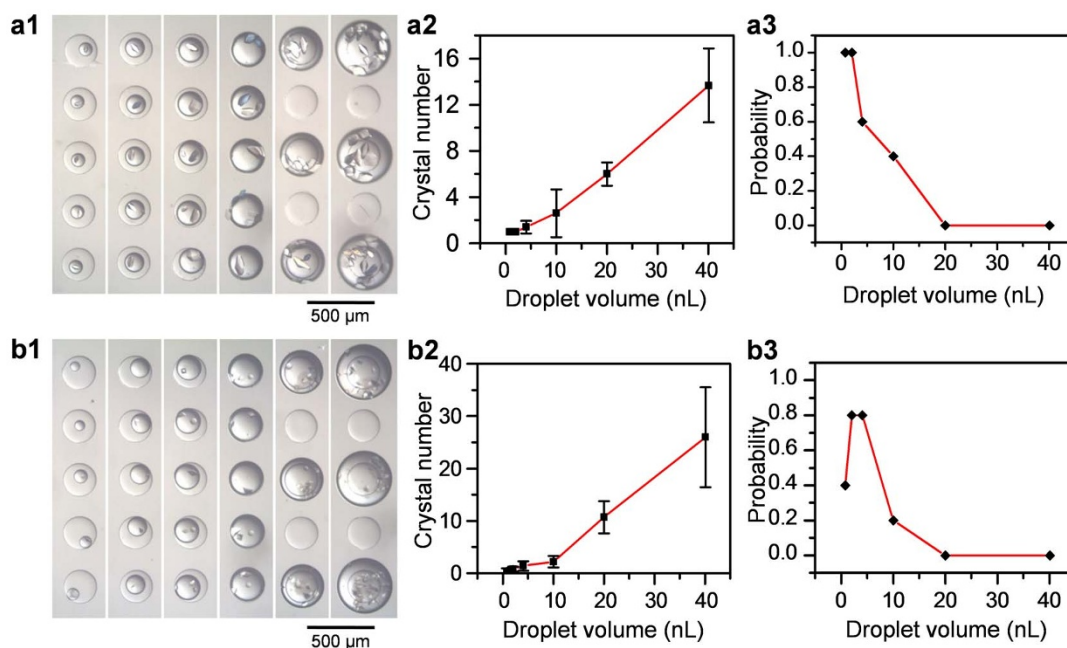
Figure 5 | Effects of droplet volume on protein crystallization. Microscopic images showing crystallization of (a1) lysozyme and (b1) thaumatin in droplets with volumes of 0.84 nL, 2.04 nL, 4.02 nL, 4.08 nL, 10.02 nL, 20.04 nL, and 40.08 nL. Scale bar is 500 μm. The relationship between droplet volumes and the number of protein crystals in each droplet for (a2) lysozyme and (b2) thaumatin. The relationship between frequency of single crystal formed in droplets and droplet volume for (a3) lysozyme and (b3) thaumatin. Crystallization conditions: for lysozyme, 50 mg/mL in 0.1 M NaAc buffer (pH 4.6); Mixing ratio of 1 : 1 with 10%(w/v) NaCl in 0.1 M NaAc (pH 4.6); for thaumatin, 30 mg/mL in 0.1 M ADA buffer (pH 6.5); Mixing ratio of 1 : 1 with 2 M sodium/potassium tartrate in 0.1 M HEPES (pH 7.5).

limited supplies. In the experiments of sparse matrix screening and volume effect investigation, we also demonstrated that small-volume (picoliter or nanoliter) trials can be gradually scaled up to large volume (microliter) trials without significant changing of crystallization condition, which would allow crystals obtained from the droplet robot to be directly used for data collection with synchrotron radiation. The semi-open structure of the droplet array system grants easy crystal harvesting by simply extracting the droplets through oil layer with a capillary. Further optimization to the droplet robot (for example, performing liquid-handling in parallel and expanding to more protein crystallization modes) will further improve the throughput and enhance the scope and capability for protein crystallization in the future.

Methods

Assembling of the droplet robot. The droplet robot was assembled with four parts: a high-precision syringe pump (PHD 2000, Harvard Apparatus, Holliston, USA) with a 1-μL syringe (7000 series, Hamilton, Reno, USA) for liquid metering; a tapered capillary (150-μm i.d., 250-μm o.d., Reafine Chromatography, Handan, China) was used to aspirate and dispense droplets; a high-density nanowell-array chip with a frame for droplet storage and incubation; an x-y-z translational stage (PSA series, Zolix, Beijing, China) was used to precisely control the movement of the microchip and 384-well plates relative to the tapered capillary. The capillary was connected with the 1-μL syringe fixed on the syringe pump via a Tygon tube. The syringe pump and the x-y-z translational stage were synchronously controlled using a program written with Labview (Labview 8.0, National Instruments, Austin, USA). Droplet manipulation process was monitored and recorded with a stereomicroscope (SMZ 850T, Touptek, Hangzhou, China) equipped with a CCD camera (HV3151UC, Daheng Imavision, Beijing, China). The syringe pump was operated with a flow rate of 200 nL/min under volume mode. The x-y-z translational stage was set at an initial velocity of 10 mm/s, an acceleration of 30 mm/s², and an uniform velocity of 30 mm/s.

Fabrication of microchip and tapered capillary. Nanowell-array chips were fabricated using standard photolithography and wet chemical etching techniques from glass plates with chromium and photoresist coating (Shaoguang Microelectronics, Changsha, China) as described elsewhere[28]. After an etching time of 60 min at 40°C in an etching solution (HF/NH₄F/HNO₃, 1.0/0.5/0.75 M), a nanowell array with each well size of ca. 80-μm depth, 260-μm diameter, and 400-μm center-to-center distance between adjacent wells was fabricated on a glass plate. A glass

frame with a thickness of 1.6 mm was glued on each nanowell-array chip for containing cover oil. The tapered capillary was prepared by tapering a capillary to a final tip size of ca. 20-μm i.d. and 30-μm o.d. using a micropipette puller (P2000/F, Sutter instrument, Novato, USA). Both the microchip and capillary were treated with 1% octadecyltrichlorosilane (OTCS, Sigma, St. Louis, USA) in isooctane (v/v) to make their surfaces hydrophobic[28].

Sparse matrix screening of protein crystallization. A commercial kit (Index HT, Hampton Research, Aliso Viejo, USA) containing 96 different precipitants was used to screen the crystallization conditions of lysozyme and xylanase. Before droplet generation, a microchip was mounted on the x-y-z translational stage and then covered with a layer of mineral oil in the frame. The syringe and capillary were filled with water to remove air inside them. A plug of mineral oil with a length of ca. 1-mm was aspirated into the capillary tip as carrier oil for separating the water inside the capillary from aspirated crystallization samples and reagents. Each precipitant droplet was generated by allowing the capillary tip to be inserted into the 384-well plate, aspirating 2.01-nL precipitant solution into the capillary tip, and then depositing it into a definite nanowell with a distance d_1 of 100 μm to form a water-in-oil droplet. Three droplets were produced for each precipitant condition. After all the precipitant droplets were generated, protein solution with a volume of 580 nL was aspirated into the capillary and then sequentially dispensed on the top of each precipitant droplet with a fixed dispensing volume of 2.01 nL. The distance d_2 was set as 150 μm to allow the dispensed protein droplets contact with preformed droplets. The dispensed protein droplets could quickly fuse with precipitant droplets and mix with them to form crystallization reactors. Finally, the microchip was sealed with a glass plate and incubated in a thermostat. The thermostat was set at 4°C for lysozyme and 16°C for all other proteins. For crystal identification, the droplet array was imaged on an inverted microscope, which was operated with the illumination of polarized light or under the mode of differential interference contrast (DIC) microscopy. To further discriminate the protein crystals from salt crystals, we used a metal needle to crush the crystal, because the protein crystals are commonly softer than salt crystals due to their crystal packing characteristics. The identified crystallization precipitants were validated in scale-up experiments using standard 96-well microbatch plates (Hampton Research, Aliso Viejo, USA).

Determination of 2D protein phase diagram. For lysozyme, stock protein solution (100 mg/mL in 0.1 M NaAc buffer (pH 4.6)), stock precipitant solution (NaCl, 10% (w/v) in 0.1 M NaAc buffer (pH 4.6)), and its buffer solution (NaAc buffer (pH 4.6)) were prepared. For thaumatin, stock protein solution (100 mg/mL in 0.1 M ADA buffer (pH 6.5)), stock precipitant solution (2 M sodium potassium tartrate in 0.1 M HEPES (pH 7.5)), and its buffer solution (0.1 M HEPES (pH 7.5)) were used. The nanowell array chip and the capillary were pre-prepared using the procedures as described above. To generate a 9 × 9 droplet array for a protein phase diagram
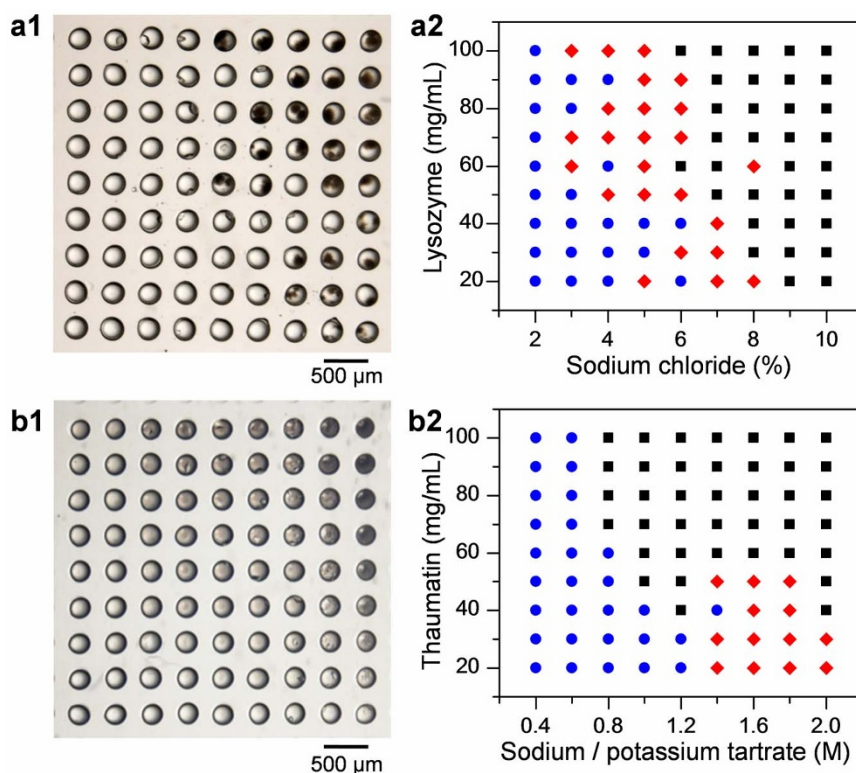
Figure 6 | Automated determination of 2D protein phase diagrams with droplet arrays. Typical microscopic images of 2D droplet array for (a1) lysozyme and (b1) thaumatin, visually exhibiting different protein phase behaviors at given chemical conditions. Phase diagrams of (a2) lysozyme and (b2) thaumatin show the phase regions of undersaturation (●), metastable or nucleation (◆), and precipitation (■).

determination, protein stock solution with a volume of 205 nL was first aspirated into the capillary and sequentially dispensed into nanowells to form a 9 × 9 array of protein droplets with different volumes ranging from 0.84 nL to 4.2 nL (Table S1). The distance d_1 was set as 60 μm to allow the dispensed droplets contact the chip surface and release from the capillary tip. Droplet volumes in each line were the same, and the volumes were linearly increased from the bottom line to the top line with an increment of 0.42 nL. Then, the buffer solution with a volume of 275 nL was aspirated and sequentially added into each droplet with distance d_2 of 150 μm and volumes as shown in Table S1. Finally, precipitant stock solution was dispensed into the preformed droplets with programmable volumes (Table S1). The final volume of each droplet containing protein, buffer, and precipitant solutions was 8.4 nL. The microchip was also sealed and incubated for crystal growth and detection.

1. Kendrew, J. C. *et al.* 3-dimensional model of the myoglobin molecule obtained by x-ray analysis. *Nature* **181**, 662–666 (1958).
2. Li, Y. *et al.* FtsZ protofilaments use a hinge-opening mechanism for constrictive force generation. *Science* **341**, 392–395 (2013).
3. Schmid, M. B. Seeing is believing: the impact of structural genomics on antimicrobial drug discovery. *Nat. Rev. Microbiol.* **2**, 739–746 (2004).
4. Lamers, M. H. *et al.* The crystal structure of DNA mismatch repair protein MutS binding to a G center dot T mismatch. *Nature* **407**, 711–717 (2000).
5. Blundell, T. L., Jhoti, H. & Abell, C. High-throughput crystallography for lead discovery in drug design. *Nat. Rev. Drug Discov.* **1**, 45–54 (2002).
6. Burley, S. K. *et al.* Structural genomics: beyond the human genome project. *Nat. Genet.* **23**, 151–157 (1999).
7. Newby, Z. E. R. *et al.* A general protocol for the crystallization of membrane proteins for X-ray structural investigation. *Nat. Protoc.* **4**, 619–637 (2009).
8. Hansen, C. L., Skordalakes, E., Berger, J. M. & Quake, S. R. A robust and scalable microfluidic metering method that allows protein crystal growth by free interface diffusion. *P. Natl. Acad. Sci. U.S.A.* **99**, 16531–16536 (2002).
9. Chayen, N. E. Turning protein crystallisation from an art into a science. *Curr. Opin. Struc. Biol.* **14**, 577–583 (2004).
10. Chayen, N. E. & Saridakis, E. Protein crystallization: from purified protein to diffraction-quality crystal. *Nat. Methods* **5**, 147–153 (2008).
11. Benvenuti, M. & Mangani, S. Crystallization of soluble proteins in vapor diffusion for X-ray crystallography. *Nat. Protoc.* **2**, 1633–1651 (2007).
12. Hansen, C. & Quake, S. R. Microfluidics in structural biology: smaller, faster... better. *Curr. Opin. Struc. Biol.* **13**, 538–544 (2003).
13. Li, L. & Ismagilov, R. F. Protein crystallization using microfluidic technologies based on valves, droplets and SlipChip. *Annu. Rev. Biophys.* **39**, 139–158 (2010).
14. Chayen, N. E., Shaw Stewart, P. D., Maeder, D. L. & Blow, D. M. An automated system for micro-batch protein crystallization and screening. *J. Appl. Crystallogr.* **23**, 297–302 (1990).
15. Stevens, R. C. High-throughput protein crystallization. *Curr. Opin. Struc. Biol.* **10**, 558–563 (2000).
16. Rose, D. Microdispensing technologies in drug discovery. *Drug Discov. Today* **4**, 411–419 (1999).
17. Cleveland, P. H. & Koutz, P. J. Nanoliter dispensing for uHTS using pin tools. *Assay Drug Dev. Technol.* **3**, 213–225 (2005).
18. Wong, E. Y. & Diamond, S. L. Advancing microarray assembly with acoustic dispensing technology. *Anal. Chem.* **81**, 509–514 (2009).
19. Hansen, C. L., Sommer, M. O. A. & Quake, S. R. Systematic investigation of protein phase behavior with a microfluidic formulator. *P. Natl. Acad. Sci. U.S.A.* **101**, 14431–14436 (2004).
20. Lau, B. T. C., Baitz, C. A., Dong, X. P. & Hansen, C. L. A complete microfluidic screening platform for rational protein crystallization. *J. Am. Chem. Soc.* **129**, 454–455 (2007).
21. Zheng, B., Roach, L. S. & Ismagilov, R. F. Screening of protein crystallization conditions on a microfluidic chip using nanoliter-size droplets. *J. Am. Chem. Soc.* **125**, 11170–11171 (2003).
22. Zheng, B. & Ismagilov, R. F. A microfluidic approach for screening submicroliter volumes against multiple reagents by using preformed arrays of nanoliter plugs in a three-phase liquid/liquid/gas flow. *Angew. Chem. Int. Edit.* **44**, 2520–2523 (2005).
23. Du, W. B., Li, L., Nichols, K. P. & Ismagilov, R. F. SlipChip. *Lab Chip* **9**, 2286–2292 (2009).
24. Li, L., Du, W. B. & Ismagilov, R. F. Multiparameter screening on slipchip used for nanoliter protein crystallization combining free interface diffusion and microbatch methods. *J. Am. Chem. Soc.* **132**, 112–119 (2010).
25. Selimovic, S., Gobeaux, F. & Fraden, S. Mapping and manipulating temperature-concentration phase diagrams using microfluidics. *Lab Chip* **10**, 1696–1699 (2010).
26. Shim, J. U., Cristobal, G., Link, D. R., Thorsen, T. & Fraden, S. Using microfluidics to decouple nucleation and growth of protein crystals. *Cryst. Growth Des.* **7**, 2192–2194 (2007).
27. Leung, K. *et al.* A programmable droplet-based microfluidic device applied to multiparameter analysis of single microbes and microbial communities. *P. Natl. Acad. Sci. U.S.A.* **109**, 7665–7670 (2012).
28. Zhu, Y., Zhang, Y. X., Cai, L. F. & Fang, Q. Sequential operation droplet array: an automated microfluidic platform for picoliter-scale liquid handling, analysis, and screening. *Anal. Chem.* **85**, 6723–6731 (2013).

29. Du, W. B., Sun, M., Gu, S. Q., Zhu, Y. & Fang, Q. Automated microfluidic screening assay platform based on DropLab. *Anal. Chem.* **82**, 9941–9947 (2010).

30. Gu, S. Q. *et al.* Multifunctional picoliter droplet manipulation platform and its application in single cell analysis. *Anal. Chem.* **83**, 7570–7576 (2011).

31. Baret, J. C. Surfactants in droplet-based microfluidics. *Lab Chip* **12**, 422–433 (2012).

32. Zheng, B., Tice, J. D., Roach, L. S. & Ismagilov, R. F. A droplet-based, composite PDMS/glass capillary microfluidic system for evaluating protein crystallization conditions by microbatch and vapor-diffusion methods with on-chip X-ray diffraction. *Angew. Chem. Int. Edit.* **43**, 2508–2511 (2004).

33. Dolega, M. E. *et al.* Iterative operations on microdroplets and continuous monitoring of processes within them; determination of solubility diagrams. *Lab Chip* **12**, 4022–4025 (2012).

Acknowledgments

Author contributions

Y.Z. and L.Z. built the platform, fabricated microchips and performed the experiments. Y.Z. and L.Z. has the equal contribution to this work. R.G. and H.C. purified the membrane protein and performed the conventional crystallization experiments. Y.Z., L.Z., R.G., S.Y. and Q.F. processed the data and drafted the manuscript. Q.F. conceived the project and led the research process. All authors discussed the results and approved on the manuscript.

Additional information

Supplementary information accompanies this paper at http://www.nature.com/scientificreports

Competing financial interests: The authors declare no competing financial interests.

How to cite this article: Zhu, Y. *et al.* Nanoliter-Scale Protein Crystallization and Screening with a Microfluidic Droplet Robot. *Sci. Rep.* **4**, 5046; DOI:10.1038/srep05046 (2014).